Kinetic Energy Driven Ferromagnetic Insulator

Jinyuan Ye,[1,2,3] Yuchi He,[4,*] and Congjun Wu[2,3,5,6,†]
[1]Department of Physics, Fudan University, Shanghai 200433, China
[2]New Cornerstone Science Laboratory, Department of Physics, School of Science, Westlake University, Hangzhou 310024, Zhejiang, China
[3]Institute of Natural Sciences, Westlake Institute for Advanced Study, Hangzhou 310024, Zhejiang, China
[4]Rudolf Peierls Centre for Theoretical Physics, Clarendon Laboratory, Parks Road, Oxford OX1 3PU, United Kingdom
[5]Institute for Theoretical Sciences, Westlake University, Hangzhou 310024, Zhejiang, China
[6]Key Laboratory for Quantum Materials of Zhejiang Province, School of Science, Westlake University, Hangzhou 310024, Zhejiang, China

(Received 31 October 2024; revised 9 January 2026; accepted 23 January 2026; published 27 February 2026)

We construct a minimal model of interacting fermions establishing a ferromagnetic insulating phase. It is based on the Hubbard model on a trimerized triangular lattice in the regime of $t \gg |t'| > 0$ with t and t' the intra- and intertrimer hopping amplitudes, respectively. At the $\frac{1}{3}$-filling, each trimer becomes a triplet spin-1 moment, and the intertrimer superexchange is ferromagnetic with $J = -\frac{2}{27}(t'^2/t)$ in the limit of $U/t = +\infty$. As U/t becomes finite, the antiferromagnetic superexchange competes with the ferromagnetic one. The system enters into a frustrated antiferromagnetic insulator when $\lambda > U/t \gg 1$ where λ is a constant at the order of 10. In contrast, a similar analysis to the trimerized Kagome lattice shows that only the antiferromagnetic superexchange exists at $\frac{1}{3}$-filling.

DOI: 10.1103/mg2p-3f4k

The mechanism of ferromagnetism is a long-standing problem of strong correlation physics [1]. The driving force of itinerant FM is often thought to be the direct exchange among electrons with the same spin to reduce the interparticle repulsion. Spin polarization pays a large cost of kinetic energy due to Pauli's exclusion principle, such that in most situations, fermions would rather develop unpolarized but highly correlated many-body ground states than be polarized. Nevertheless, a few rigorous results have been established: The Nagaoka theorem proves that the infinite U Hubbard model at half-filling with doping only a single hole develops FM [2,3], for a bipartite lattice regardless of the sign of hopping and for a nonbipartite lattice with positive hopping. Another class of theorems of FM rely on the flat-band structure of line graphs in which the kinetic energy is suppressed to zero [4–7]. It is also shown that FM could remain stable under certain conditions even when the band structure becomes nonsingular [8]. Furthermore, a series of theorems prove that Hund's interaction combined with the quasi-one-dimensional band structure lead to itinerant FM in the multiorbital Hubbard model over a large region of filling factors [9]. The Curie-Weiss metal state and the ferromagnetic (FM) criticality are accurately studied by quantum Monte Carlo simulations free of the sign problem [10].

On the other hand, Mott insulators are typically dominated by antiferromagnetic (AFM) superexchange. Upon doping, they may serve as the parent compounds of high T_c superconductors. In frustrated systems, such as triangular and Kagome lattices, the AFM spin alignment of each bond cannot be simultaneously satisfied due to the geometry constraint. An incredibly rich and complex nature of quantum magnetism manifests [11–15], leading to exotic states of spin liquid [16–18]. Owing to the complexity of frustrated magnets, the cluster model approach is widely employed for theoretical studies. It extends beyond the concept of individual sites, focusing instead on well-defined clusters of atoms as the fundamental units. Unequal coupling strengths cause electrons to localize inside these clusters, rather than on individual atomic sites. The localized degrees of freedom can be effectively described in terms of molecular orbitals, giving rise to what are often referred to as *molecules in solids* [19]. Coupled clusters can form cluster Mott insulators [20–24]. Experimentally, such clusters in the triangular lattice material of $LiVO_2$ [25], and in Kagome lattice materials of Nb_3Cl_8 [26] and the Mo_3O_8 family of compounds [27–31].

It would be nontrivial to unify FM and AFM in the same system regarding their very different origins. In this Letter,

*Contact author: yuchi.he@physics.ox.ac.uk
†Contact author: wucongjun@westlake.edu.cn

we find the transition from an AFM insulator to an FM one simply as increasing interaction strengths. It is based on the Hubbard model defined in a trimerized triangular lattice at the $\frac{1}{3}$-filling in the strong coupling regime $U \gg t \gg |t'|$. Two electrons in each trimer form a spin-1 triplet at $t > 0$. The intertrimer hopping generates both FM and AFM superexchanges: The former involves intermediate excitations free of double occupancy with the energy cost of t analogous to the case of charge-transfer insulators, while the latter generates double occupancy with the energy cost of U similar to the case of Mott insulators. At $U/t = +\infty$, the FM exchange dominates while it switches to the AFM one at around $U/t \approx 13 \sim 15$, as confirmed by our density-matrix-renormalization-group [32–37] (DMRG) simulations. The FM insulating state remains robust by threading a weak staggered flux pattern of ϕ, and it becomes an FM metal at small doping levels. In contrast, as for the trimerized Kagome lattice, the intertrimer exchange is always AFM-like. Our mechanism is different from the orbital-active Mott insulators in which FM exchange could appear according to Kugel-Khomskii physics [38]. In that case, the overall nature of superexchange remains antiferro, either ferro in orbital and antiferro in spin *or* antiferro in orbital and ferro in spin.

Model Hamiltonian—We consider the Hubbard model $H = H_0 + H'$ defined in a trimerized triangular lattice as illustrated in Fig. 1(a),

$$H_0 = t\sum_{\langle ij\rangle}\left\{c^\dagger_{i\sigma}c_{j\sigma} + \text{H.c.}\right\} + \sum_i U n_{i,\uparrow}n_{i,\downarrow},$$
$$H' = t'\sum_{\langle\langle i'j'\rangle\rangle}\left\{c^\dagger_{i'\sigma}c_{j'\sigma} + \text{H.c.}\right\}, \quad (1)$$

where H_0 is the intratrimer Hamiltonian and H' describes the intertrimer hopping; $\langle ij\rangle$ and $\langle\langle i'j'\rangle\rangle$ represent the intra- and intertrimer bonds, respectively. To establish FM below half-filling, it is crucial to have $t > 0$ due to the absence of particle-hole symmetry in nonbipartite lattices. Two neighboring trimers are connected by two links; hence, the superexchanges between them are insensitive to the sign of t'.

The free-band structure of the trimerized configuration is depicted in Supplemental Material Sec. A [39]. Since $t \gg |t'|$, three intratrimer states are solved as orbitals: The lower two are degenerate with the energy of $E = -t$ and the upper with $E = 2t$. They are broadened into three bands whose widths are proportional to $|t'|$. The lower two bands overlap and are separated from the upper one. The band gap Δ_b between them is at the order of t at $|t'/t| \ll 1$, while it closes at $t'/t = 3/4$.

Below we consider the commensurate filling of $\frac{1}{3}$, i.e., two fermions per trimer. The lower two bands are effectively half-filled; hence, it should be metallic in the weak coupling regime of $U/t' \lesssim 1$. In contrast, the strong coupling regime is characterized by $\min(U, t) \gg t'$, in which the correlated insulating states appear. The intertrimer hopping generates virtual excitations involving one or three fermions in a trimer. The dependence of E_{ex} on t and U here are depicted in Figs. 2(a) and 2(b), respectively (see Supplemental Material Sec. B [39]). Excitations with $E_{\text{ex}} \sim t$ lead to the FM superexchange in the regime of $U \gg t \gg t'$. As U/t lowers, the AFM superexchange becomes dominant as in the usual Mott insulators, and the excitations are characterized by double occupancy with $E_{\text{ex}} \sim U$. The evolution from the FM to AFM superexchange is explained below.

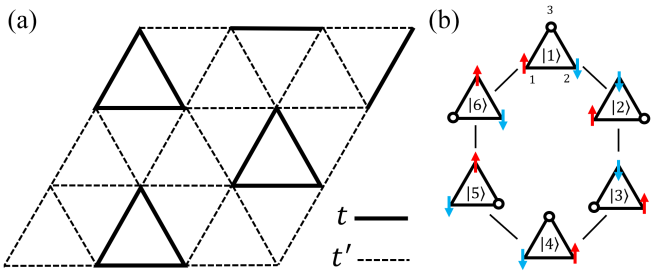

FIG. 1. (a) The trimerized triangular lattice with hopping strengths—the intratrimer hopping t and the intertrimer hopping t' represented by the solid and dashed lines, respectively. Each trimer is filled with two electrons. (b) The bases of the sector with $S_{\text{tot}} = 0$ are generated by the hole's hopping around the trimer, sequentially denoted as $|1\rangle = c^\dagger_{1\uparrow}c^\dagger_{2\downarrow}|\Omega\rangle$, $|2\rangle = c^\dagger_{3\downarrow}c^\dagger_{1\uparrow}|\Omega\rangle$, $|3\rangle = c^\dagger_{2\uparrow}c^\dagger_{3\downarrow}|\Omega\rangle$, $|4\rangle = c^\dagger_{1\downarrow}c^\dagger_{2\uparrow}|\Omega\rangle$, $|5\rangle = c^\dagger_{3\uparrow}c^\dagger_{1\downarrow}|\Omega\rangle$, and $|6\rangle = c^\dagger_{2\downarrow}c^\dagger_{3\uparrow}|\Omega\rangle$.

We begin with the case of $U/t = +\infty$, which forbids the double occupancy. The Nagaoka theorem applies to the case with only a single hole in the entire system [2]. Below the dominance of the FM exchange is shown to occur at the $\frac{1}{3}$-filling.

Single trimer—At $t' = 0$ the system is reduced to disconnected trimers. When the trimer is filled with two electrons, it is sufficient to consider the sector of $S_{\text{tot},z} = 0$ within a trimer based on the SU(2) symmetry. This local Hilbert space contains six bases denoted as $|m\rangle (m = 1 \sim 6) : |1\rangle = c^\dagger_{1\uparrow}c^\dagger_{2\downarrow}|\Omega\rangle$ with $|\Omega\rangle$ denoting the vacuum state, and the other states $|m\rangle$ are generated as the hole hops around the trimer in a clockwise way as shown in Fig. 1(b). In this convention, $|m\rangle$ and $|m+3\rangle$ correspond to a pair of states by flipping two spins. Applying H_0 on $|m\rangle$, it yields $H_0|m\rangle = -t(|m-1\rangle + |m+1\rangle)$, where m is defined as modulo 6.

Remarkably, this intratrimer two-electron problem exhibits a sixfold rotational symmetry. This can be mapped to a rolling motion problem: The pair of spins represents a two-tooth external gear, and the trimer behaves as a three-tooth internal gear. Since rolling is a combination of translation and rotation, one round is insufficient to restore the configurations of both degrees of freedom back to the

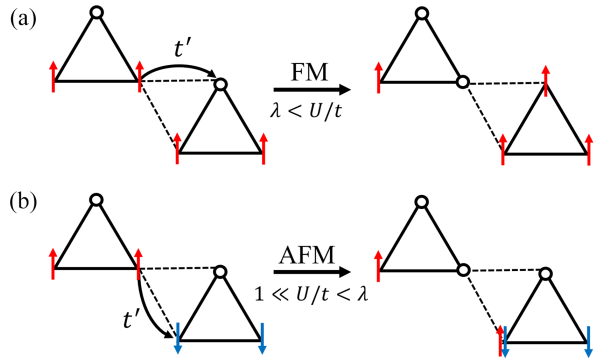

FIG. 2. Particle-hole excitations leading to (a) the FM superexchange at $U/t > \lambda$ and (b) the AFM one at $\lambda > U/t \gg 1$, respectively, with the transition value $\lambda \sim 10$. For the FM case, the excitation energy $E_{\mathrm{ex}} \sim t$ with only single occupations analogs to charge-transfer insulators, while $E_{\mathrm{ex}} \sim U$ for the AFM case manifesting Mott physics characterized by the double occupancy.

initial ones. Instead, the minimal requirement to a periodicity requires rolling two rounds. Consequently, this problem is mapped to a single-body problem moving around a hexagon. It is interesting that the effective orbital angular momentum here is modulo 6 instead of 3, exhibiting a fractionalization behavior.

The eigenstates for the single trimer problem in the sector of $S_{\mathrm{tot},z} = 0$ are solved as

$$|k_n\rangle = \frac{1}{\sqrt{6}} \sum_n e^{ik_n m} |m\rangle, \tag{2}$$

with the energy spectrum, $E_n = -2t \cos k_n$, where $k_n = (n/3)\pi$ with $n = 0, \pm 1, \pm 2, 3$. The states with $n = 0, \pm 2$ are symmetric under the operation $m \to m + 3$; hence, they are spin triplet. In contrast, the other states with odd values of n are spin singlet. For $t > 0$, the ground state with $n = 0$ is a spin triplet, and the lowest excitations are a pair of singlets with a gap of t.

Trimerized triangular lattice—Next consider the case of $0 < |t'|/t \ll 1$. Since the trimer ground state is spin-1, H' generates intertrimer superexchanges and lifts the degeneracy. The weakly coupled trimers are effectively described by the spin-1 Heisenberg model in a triangular lattice where one site represents a trimer. The effective exchange Hamiltonian reads

$$H_{ex} = J \sum_{\langle ij \rangle} \mathbf{S}_i \cdot \mathbf{S}_j + C, \tag{3}$$

where $\mathbf{S}_i$ represents the total spin of the trimer i, J is the exchange energy, and C is an energy constant, which will be determined below.

The J turns out to be FM as calculated via the second-order degenerate perturbation theory. The total spin of two neighboring trimers lie in three channels of $S_{\mathrm{tot}} = 2$, 1, and 0. The energy gains in these channels are shown in Supplemental Material Sec. C [39], yielding that $\Delta E^{(2)}/(t'^2/t) = -\frac{10}{27}, -\frac{6}{27}, -\frac{4}{27}$, respectively. Comparing to Eq. (3), we arrive at

$$J = -\frac{2}{27}\frac{t'^2}{t}, \qquad C = 4J. \tag{4}$$

Therefore, the $\frac{1}{3}$-filled trimerized triangular lattice is in the FM insulating state in the limit of $U \to \infty$ and $t'/t \ll 1$ due to the FM superexchange.

Flux threading—Next consider the effect of a trimerized triangular lattice with a staggered flux pattern $\pm\phi$ threading each plaquette as shown in Supplemental Material Sec. C [39]. Correspondingly, the intratrimer hopping amplitude t and the intertrimer one t' are modified as $te^{\pm i(\phi/3)}$ and $t'e^{\pm i(\phi/3)}$, where the signs $\pm$ are determined by whether the hopping is along or against the flux winding, respectively. The flux modifies the energy spectrum of the six intratrimer two-electron states as

$$E_n = -2t \cos\left(k_n + \frac{\phi}{3}\right), \tag{5}$$

where ϕ is defined as modulo 2π. Nevertheless, the spectral flow indicated by Eq. (5) shows that the dispersion returns back at $\phi = \pi$, i.e., $n \to n + 1$ (modulo 6), but switching triplet and singlet states.

The FM exchange described in Eq. (3) remains robust at small values of $|\phi| < (\pi/2)$ since the intratrimer ground state remains the triplet $|k_0\rangle$. Nevertheless, J is reduced: The second-order perturbation calculation shows that at $|\phi| < (\pi/2)$ the flux dependence of $J(\phi)$ reads

$$J(\phi) \approx J\left(1 - \frac{7}{54}\phi^2\right). \tag{6}$$

A more accurate expression is obtained as $J(\phi) = -(t'^2/18t)[\cos(2\phi/3)\ \cos(\phi/3)]/\{\cos[(\phi/3) + (\pi/6)]\ \cos[(\phi/3) - (\pi/6)]\}$.

When ϕ reaches $\pm(\pi/2)$, the intratrimer singlet and triplet states become degenerate. According to the decomposition rule of the SU(2) representations, two trimers result in six spin channels: One set of quintet ($S_{\mathrm{tot}} = 2$), three sets of triplet ($S_{\mathrm{tot}} = 1$), and two sets of singlet ($S_{\mathrm{tot}} = 0$). The lowest and highest energy states are both spin singlets (see Supplemental Material Sec. C [39]): The former is the direct-product state of two trimer singlets, and the latter is the entangled one built up by two trimer triplets, exhibiting the energies of $\Delta E^{(2)}_{s,1} = -(83t'^2/108\sqrt{3}t)$ and $\Delta E^{(2)}_{s,2} = -(5t'^2/12\sqrt{3}t)$, respectively. They do not mix at the level of the second-order perturbation theory; nevertheless, a small mixing could occur at a high order. This means that as $|\phi|$ increases from 0 to $(\pi/2)$ the ground state

of the entire lattice changes from the spin fully polarized state to the direct product state of the singlet of each trimer. The transition between two different types of ground states will be deferred to a future research.

Phase transitions by tuning t' and U—We now consider finite values of U, which generates the competition between AFM and FM exchanges. For simplicity only the case of $\phi = 0$ is considered here. The intratrimer ground states are a set of spin-1 triplets as long as $U > 0$ [39], in contrast to the case of a square where the ground state becomes spin-$\frac{3}{2}$ at a large value of $U/t \geq 18.7$ [40]. The detailed calculation of the superexchange coupling J between two neighboring spin-1 trimers at finite values of U is presented in Supplemental Material Sec. D [39], yielding

$$J = -\frac{2}{27}\frac{t'^2}{t} + \frac{62}{81}\frac{t'^2}{U}, \tag{7}$$

where $1 \ll U/t < \infty$ is assumed. The first term in Eq. (7) arises from the FM superexchange as explained before, and the second one is the AFM superexchange involving doubly occupied intermediate states. The overall value of J switches from FM to AFM approximately at $U_F/t \approx 10.3$ at which $J = 0$. Around $J = 0$, high-order superexchanges would be important.

We compute the phase diagram of the trimerized triangular lattice model at the $\frac{1}{3}$-filling in $t'/t - U/t$ parameter space, as shown in Fig. 3(a). At $t'/t \geq 3/4$, the band gap closes and the system remains metallic even at large values of U/t. Our main purpose here is to study the competition between FM and AFM superexchanges in the insulating states and leave the metallic state for future studies; hence, only the parameter range of $0 < t'/t \leq 0.6$ will be explored here. DMRG simulations are performed to a 72-site system. The FM superexchange dominates over the AFM one, leading to a fully polarized FM insulating state when U/t is larger than a t'/t-dependent critical value U_F/t as indicated by the solid line. As t' increases, higher order virtual hopping processes become more prominent and then larger values of U_F/t are required to establish the FM phase. As an example, the transition to spin polarized states at $t'/t = 0.2$ is shown in Fig. 3(b), indicating $U_F/t \approx 14$, and the corresponding single-electron gap Δ is shown in Fig. 3(c). There may exist intermediate phases near the transition, which will be deferred to future studies.

As U/t lowers further, the system is expected to transition into the gapless metallic phase in the thermodynamic limit. The precise location of this phase boundary is challenging due to the intrinsic difficulty of many-body simulations. For this we employ the infinite DMRG method for a quasi-one-dimensional system. The equal-time single-electron Green's functions decay exponentially in the AFM state, whose decaying length ξ_e's are extracted as shown in Supplemental Material Sec. I [39]. As the interaction

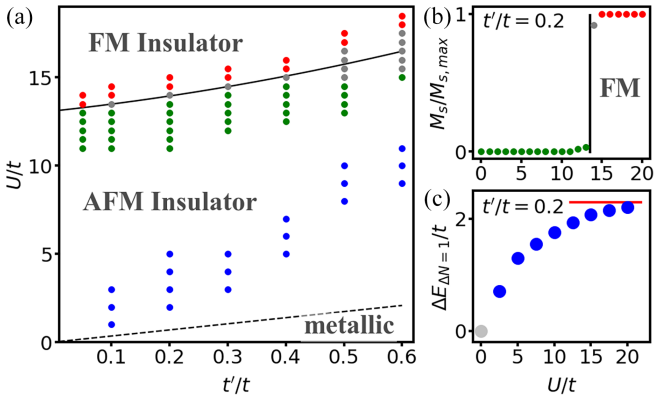

FIG. 3. (a) The phase diagram at the $\frac{1}{3}$-filling for $0 < t'/t \leq 0.6$. DMRG calculations are applied for the system on a tilted cylinder with the size of $L_x \times L_y \times 3$ to determine the boundary between the fully spin-polarized FM insulating state and the unpolarized AFM one, which is marked by a solid line. The AFM-FM transition is determined based on $L_x = 6$, $L_y = 4$. The data of $L_x = \infty$ and $L_y = 3$ are also calculated yielding similar results. The decay length ξ_e is extracted from the single-electron Green's function by extending the system to the quasi-one-dimensional limit of $L_x \to \infty$ (see Supplemental Material Sec. G). Charge localizations are found down to certain values of U, and the data with ξ_e less than the intertrimer distance $\sqrt{3}a$ are marked by blue dots for reference. The metal-insulator transition boundary (black dashed line) is estimated from the relation $U_c/W \approx \sqrt{3}/2$, where W is the free bandwidth. (b) The relative spontaneous magnetization $M_s/M_{s,max}$, with $M_s = \sqrt{\langle S^2_{tot}\rangle}$ and $M_{s,max} = \sqrt{S_{max}(S_{max}+1)}$ where $S_{max} = L_x \times L_y$ equals to the number of trimers. It reaches 1 at $U/t \approx 14$, confirming full polarization. (c) The single-electron gap, defined as $\Delta = E^{GS}_{N=49} + E^{GS}_{N=47} - 2E^{GS}_{N=48}$, exhibits nonzero values except at $U = 0$. The $U = 0$ result has exactly zero gap because there are degenerate single-particle states at Fermi energy. The red solid line is the band gap when electrons are fully spin polarized for comparison. The deviation in FM region is due to the fact that spins remain fully polarized for doping a hole but partially flip when adding an electron.

strength further lowers below the critical value of U_c/t, the single-electron gap closes and the system enters the metallic phase. According to the self-consistent solution to the equation of motion of Green's function [41], an estimation of $U_c/W \gtrsim \sqrt{3}/2$ is expected as marked in Fig. 3(a), where W is the band width determined by t'/t (see Supplemental Material Sec. E). Certainly, this method only yields a rough estimation, which cannot fully capture the correlation effect. A precise determination of the phase boundary of the metal-insulator transition at $\frac{1}{3}$-filling is beyond the scope of this Letter.

Discussions—We explore the universality underlying the above mechanism to FM, including the formation of the molecular-type (intratrimer) high-spin moment, and the intermolecular (intertrimer) FM coherence arising from the

kinetic energy gain via superexchange interactions. When two fermions fill the doubly degenerate intratrimer levels, they form a spin-1 moment at $U > 0$. This Hund's rule type of physics is a reminiscence of the flat-band FM in the limit of few sites. Trimer molecules become Mott insulating when the intertrimer hopping $|t'| \ll t, U$. The kinetic energy is lowered due to the intertrimer virtual hoppings leading to superexchange interactions. If the intermediate excitations generated by virtual hoppings are dominated by doubly occupied sites, the resulting superexchange is AFM-like. Since our molecular Mott-insulators are at $\frac{1}{3}$-filling, when $U \gg t$ the dominant excitations are actually free of double occupancy with excitation energies at the order of t, which is similar to charge-transfer insulators, leading to the FM superexchange.

The FM nature of superexchanges in our case becomes manifest by comparing the AFM and FM configurations of two neighboring spin-1 trimers: $S_z = \pm 1$ for each trimer, respectively, in the former case, and $S_z = 1$ for both trimers in the latter. In both cases, the intermediate excitations are free of double occupations, consisting of a 3-filled trimer and a singly filled one. In the AFM configuration, the virtual hopping processes lead to different spin configurations. They are incoherent and thus unable to optimize the kinetic energy. In contrast, similar to the Nagaoka FM, all virtual hopping processes in the case of FM configuration lead to the same fully polarized intermediate state; hence, all virtual hopping processes are coherent such that the kinetic energy gain is maximized. Hence, our description constitutes a hybrid, generalized mechanism that extends beyond the strict requirement of either Nagaoka or flat-band FM models. Experimentally, in multiorbital solid state systems, Hund's coupling often exists, promoting the formation of local high-spin moments. When there exist other low energy orbitals to host spin-polarized intermediate excitations generated by virtual hopping processes, our FM mechanism can also apply to such kinds of materials.

It would be interesting to further explore the physics by doping the $\frac{1}{3}$-filling correlated insulating state in the triangular lattice. When the FM superexchange dominates, the system will become an FM metal upon slight hole doping. The doped holes move in the background of spin-1 moments coupled by the FM superexchange, which still results in FM polarization. At $\frac{1}{4}$-filling, i.e., the case that the average fermion number in each trimer equals $\frac{3}{2}$, our preliminary simulation results show that for the value of $t'/t = 0.2$, the system has already been fully spin polarized as an FM metal at $U_F/t > 10$, which is notably lower than that at a $\frac{1}{3}$-filled insulating state. The $\frac{1}{4}$-filling can be viewed as half of the spin-1 trimers are replaced by spin-$1/2$ fermions, and the itineracy facilitates the FM coherence. The detailed study will be deferred for a future publication.

We briefly discuss the situation of $t < 0$. For a single trimer, the two-particle ground state is a spin singlet corresponding to $n = 3$ in Eq. (2). There exists a gap to the intratrimer triplet excitations at $\Delta = t$. Hence, the effective model at $\frac{1}{3}$-filling is a rotor model with the intertrimer coupling at the order of t' yielding a nonmagnetic ground state in the regime of $t' \ll t$. On the other hand, our previous studies apply to the case of the $\frac{2}{3}$-filling, since it is mapped to the $\frac{1}{3}$-filling at $t > 0$ by a particle-hole transformation.

Conclusion—We propose a mechanism to the FM insulating state in the trimerized triangular lattice, which occurs at the $\frac{1}{3}$-filling with $t > 0$ in the regime of $U \gg t \gg |t'|$. In each trimer, two electrons form spin-1 moments due to the "orbital" degeneracy and repulsive interaction. The intertrimer hopping generates superexchange couplings to lower the kinetic energy. At $U/t \to \infty$, only the FM superexchange exists, which is weakened by introducing a staggered flux pattern. As U/t becomes finite, both the FM and AFM superexchanges contribute, and the former wins over the latter around $U/t \gtrsim 15$. FM metallic state may appear upon slightly doping the $\frac{1}{3}$-filled FM insulating state. This Letter provides valuable insights into the study of quantum magnetism in strongly correlated fermion systems.

The QuSpin [42] and TeNPy [33] packages were used for the numerical studies.

Acknowledgments—We are grateful to Z. M. Pan, Y. Wang, K. Yang, and J. Zhang for valuable discussions. C. W. is supported by the National Natural Science Foundation of China under the Grants No. 12574274, No. 12234016, and No. 12550402. Y. H. is supported by European Research Council (ERC) under the European Union Horizon 2020 Research and Innovation Programme (Grant Agreement No. 804213-TMCS). This work has been supported by the New Cornerstone Science Foundation. The computation resource was provided by the Westlake HPC Center.

[1] J. Kanamori, Prog. Theor. Phys. **30**, 275 (1963).
[2] Y. Nagaoka, Phys. Rev. **147**, 392 (1966).
[3] J. O. Haerter and B. S. Shastry, Phys. Rev. Lett. **95**, 087202 (2005).
[4] A. Mielke, J. Phys. A **25**, 4335 (1992).
[5] A. Mielke, Phys. Lett. A **174**, 443 (1993).
[6] A. Mielke and H. Tasaki, Commun. Math. Phys. **158**, 341 (1993).
[7] H. Tasaki, Phys. Rev. Lett. **75**, 4678 (1995).
[8] H. Tasaki, J. Stat. Phys. **84**, 535 (1996).
[9] Y. Li, E. H. Lieb, and C. Wu, Phys. Rev. Lett. **112**, 217201 (2014).
[10] S. Xu, Y. Li, and C. Wu, Phys. Rev. X **5**, 021032 (2015).
[11] N. F. Mott, Proc. Phys. Soc. London Sect. A **62**, 416 (1949).
[12] P. Anderson, Mater. Res. Bull. **8**, 153 (1973).

[13] P. A. Lee, N. Nagaosa, and X.-G. Wen, Rev. Mod. Phys. **78**, 17 (2006).
[14] M. R. Norman, Rev. Mod. Phys. **88**, 041002 (2016).
[15] K. Kanoda and R. Kato, Annu. Rev. Condens. Matter Phys. **2**, 167 (2011).
[16] S. Sachdev, in *Quantum Magnetism*, edited by U. Schollwöck, J. Richter, D. J. J. Farnell, and R. F. Bishop (Springer, Berlin, Heidelberg, 2004), pp. 381–432.
[17] A. Vasiliev, O. Volkova, E. Zvereva, and M. Markina, npj Quantum Mater. **3**, 18 (2018).
[18] L. Savary and L. Balents, Rep. Prog. Phys. **80**, 016502 (2016).
[19] D. I. Khomskii and S. V. Streltsov, Chem. Rev. **121**, 2992 (2021).
[20] H. Yao and S. A. Kivelson, Phys. Rev. Lett. **105**, 166402 (2010).
[21] W.-Y. He, X. Y. Xu, G. Chen, K. T. Law, and P. A. Lee, Phys. Rev. Lett. **121**, 046401 (2018).
[22] J. Hu, X. Zhang, C. Hu, J. Sun, X. Wang, H.-Q. Lin, and G. Li, Commun. Phys. **6**, 172 (2023).
[23] J.-J. Jiang, Physica (Amsterdam) **540A**, 123131 (2020).
[24] G. Giri, D. Dey, M. Kumar, S. Ramasesha, and Z. G. Soos, Phys. Rev. B **95**, 224408 (2017).
[25] S. Grytsiuk, M. I. Katsnelson, E. G. v. Loon, and M. Rösner, npj Quantum Mater. **9**, 8 (2024).
[26] H. F. Pen, J. van den Brink, D. I. Khomskii, and G. A. Sawatzky, Phys. Rev. Lett. **78**, 1323 (1997).
[27] S. A. Nikolaev, I. V. Solovyev, and S. V. Streltsov, npj Quantum Mater. **6**, 25 (2021).
[28] A. Akbari-Sharbaf, R. Sinclair, A. Verrier, D. Ziat, H. D. Zhou, X. F. Sun, and J. A. Quilliam, Phys. Rev. Lett. **120**, 227201 (2018).
[29] G. Chen and P. A. Lee, Phys. Rev. B **97**, 035124 (2018).
[30] P. Gall, R. A. R. A. Orabi, T. Guizouarn, and P. Gougeon, J. Solid State Chem. **208**, 99 (2013).
[31] C. C. Torardi and R. E. McCarley, Inorg. Chem. **24**, 476 (1985).
[32] S. R. White, Phys. Rev. Lett. **69**, 2863 (1992).
[33] J. Hauschild and F. Pollmann, SciPost Phys. Lect. Notes 5 (2018).
[34] S. R. White and A. L. Chernyshev, Phys. Rev. Lett. **99**, 127004 (2007).
[35] F. Pollmann, S. Mukerjee, A. M. Turner, and J. E. Moore, Phys. Rev. Lett. **102**, 255701 (2009).
[36] V. Zauner, D. Draxler, L. Vanderstraeten, M. Degroote, J. Haegeman, M. M. Rams, V. Stojevic, N. Schuch, and F. Verstraete, New J. Phys. **17**, 053002 (2015).
[37] M. M. Rams, P. Czarnik, and L. Cincio, Phys. Rev. X **8**, 041033 (2018).
[38] A. Kugel and D. Khomskii, Sov. Phys. Usp. **25**, 231 (1982).
[39] See Supplemental Material at http://link.aps.org/supplemental/10.1103/mg2p-3f4k for additional information, which includes Refs. [34–37].
[40] J. P. Dehollain, U. Mukhopadhyay, V. P. Michal, Y. Wang, B. Wunsch, C. Reichl, W. Wegscheider, M. S. Rudner, E. Demler, and L. M. K. Vandersypen, Nature (London) **579**, 528 (2020).
[41] J. Hubbard, Proc. R. Soc. A **276**, 238 (1963).
[42] P. Weinberg and M. Bukov, SciPost Phys. **7**, 20 (2019).
[43] L. F. Tocchio, A. Montorsi, and F. Becca, Phys. Rev. Res. **3**, 043082 (2021).
[44] A. Szasz, J. Motruk, M. P. Zaletel, and J. E. Moore, Phys. Rev. X **10**, 021042 (2020).

End Matter

Extension—The studies in the main text can be easily generalized to other trimerized lattices, and for simplicity, only the case of $t' \ll t < U$ is discussed below. Figure 4(a) shows the trimerized Kagome lattice (breathing Kagome lattice) at the $\frac{1}{3}$-filling, in which two neighboring trimers only connect via one intertrimer hopping. In the case of $t > 0$, the lowest band is flat with a quadratic touching with the second one. The widths of the second and third bands are at the order of $|t'|$, and these bands are separated by the gap $\Delta_b \sim t$. When the flat band is half-filled, i.e., the $\frac{1}{6}$-filling, the system is FM, which should be stable with respect to small doping away from the $\frac{1}{6}$-filling. Nevertheless, as shown in Supplemental Material Sec. D [39], the superexchange between two neighboring trimers at the $\frac{1}{3}$-filling in the regime $U \gg t \gg t'$ is always AFM. In fact, the exchange disappears at $U/t = \infty$ because no spin-flip process takes place via a single link connecting two trimers. Finite U renders spin-flip processes feasible yielding the same Hamiltonian as Eq. (4) with the AFM exchange $J = \frac{44}{81}(t'^2/U)$. Since the trimers form a triangular lattice, the system will exhibit the 120° pattern of the AFM order.

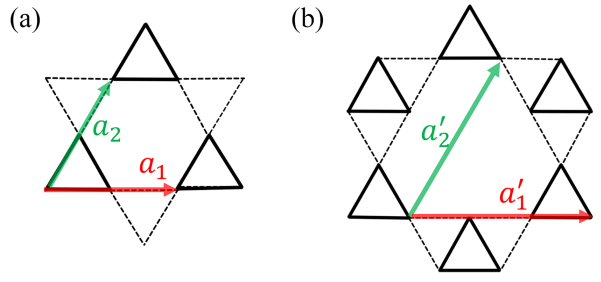

FIG. 4. (a) The trimerized Kagome lattice in which trimers form a triangular lattice. (b) The Kagome trimer lattice. Two neighboring trimers are connected via one bond in (a) and two bonds in (b), respectively.

The lattice shown in Fig. 4(b) is dubbed the Kagome trimer lattice, where trimers form a Kagome lattice and the connection between neighboring trimers is via two bonds; hence, the superexchange will be the same as in Eq. (7). Therefore, as U/t increases, the effective model will also

undergo a transition from the spin-1 AFM Heisenberg model to the FM one in the Kagome lattice.

Possible intermediate states—The superexchange J in Eq. (7) between two neighboring spin-1 trimers changes sign in the insulating states, leading to the transition from the AFM to FM states as U/t increases. Around $J = 0$, high-order exchanges including the biquadratic exchange, or ring exchange terms, could play an important role and lead to novel quantum magnetic intermediate states. These states in the thermodynamic limit may exhibit novel AFM orderings, partial FM polarization, or even more exotic quantum paramagnetic states, etc. Our DMRG data indicate that there could exist a partially polarized phase, but we cannot exclude the possibility whether the observation is a finite-size effect constrained by computational resources. It would be very interesting to further explore the possible intermediate phases, which are highly nontrivial. Nevertheless, the main point of this Letter is to provide a robust mechanism to establish a kinetic energy driven FM state. A comprehensive study of the intermediate magnetic states is a matter of accurately simulating a two-dimensional strongly correlated fermion model, which is beyond the scope of this Letter and will be deferred to future studies.

As for the metal-AFM insulator transition at a lower value of U/t, it is a notoriously difficult problem of two-dimensional strongly correlated systems in the absence of particle-hole symmetry. For the case of $t' = t$, the metal-insulator transition in the triangular lattice remains an open issue under debate in the research community [43,44]. Our trimerized case actually enriches research in this direction since the local moments in the trimerized clusters are of spin-1 instead of spin-1/2. Again, a comprehensive study of this issue is beyond the scope of the current Letter and will be deferred for future studies.